

Article ID: 1006-8775(2012) 01-0045-09

## INCONSECUTIVE “SANDWICH STRUCTURE” PATTERN FOR HIGH TEMPERATURE WARM WATER IN THE WESTERN PACIFIC WARM POOL

HUANG Fei (黄 菲)<sup>1</sup>, ZHANG Lei (张 磊)<sup>1</sup>, FAN Ting-ting (樊婷婷)<sup>1</sup>, Bin WANG (王 斌)<sup>1,2</sup>

(1. Physical Oceanography Laboratory and Key Laboratory of Ocean-Atmosphere Interaction and Climate in Universities of Shandong, Ocean University of China, Qingdao 266100 China; 2. Department of Meteorology, and International Pacific Research Center, University of Hawaii at Manoa, Honolulu, Hawaii, U.S.A.)

**Abstract:** An inconsecutive high frequency distribution with a “sandwich structure” pattern for high temperature warm water warmer than 29°C in the western Pacific warm pool (WPWP) was found using Tropical Rainfall Measuring Mission (TRMM) sea surface temperature (SST) data, a relatively high resolution data for space. This phenomenon only shows up in boreal summer (June to September), and becomes obvious when WPWP SST is higher than 29°C. As observed, East Asian summer monsoon (EASM) impinges on Philippine Islands in July, which has an important impact on the formation and maintenance of the “sandwich structure”. Winds affect the distribution of SST in two ways: one by increasing the local latent heat flux and the other by transporting cold water towards the southeast of Philippine Islands.

**Key words:** warm pool; high temperature warm water; inconsecutive frequency distribution; EASM

**CLC number:** P732      **Document code:** A      **doi:** 10.3969/j.issn.1006-8775.2012.01.005

### 1 INTRODUCTION

The western North Pacific (WNP) is an area with the highest sea temperature (ST) and heaviest rainfall in the world ocean<sup>[1]</sup>, playing a central role in the El Nino-Southern Oscillation (ENSO) phenomena<sup>[2]</sup>. The area where sea surface temperature (SST) is higher than 28°C is usually referred to as the western Pacific warm pool (WPWP). Because of the high ST and great heat content, the warm pool (WP) has great impact on the atmospheric circulation, which influences social life markedly<sup>[3]</sup>. The warm (cold) anomaly of WPWP can shift the boreal subtropical ridge northward (southward) by strengthening (weakening) convection over the Philippine Sea (PS), ulteriorly affecting East Asian climate<sup>[4]</sup>. It has been pointed out that the underlying warm pool ocean attributes much to the persistence of an anomalous Philippine Sea anticyclone which develops in the boreal fall of an El Niño year<sup>[5]</sup>.

The WP atmosphere is an important source of the atmospheric general circulation. A lot of studies

assume that atmospheric circulation is very efficient in exporting heat out of the WPA (Warm Pool Atmosphere)<sup>[6-11]</sup>. As one of the most important summer monsoon subsystems in the Asian-Pacific region<sup>[12]</sup>, East Asian summer monsoon (EASM) has great impact on WPWP. After the onset of EASM, the variation of net heat flux ( $Q_{net}$ ) and ocean circulation induced by EASM can change ST of the warm pool. In a word, WPWP is a region where the ocean and atmosphere interact with each other notably, so it is of great importance to study<sup>[13, 14]</sup>.

Though a lot of research on WP has been done before, the definition of WP boundary is not unified yet. Although SST higher than 28°C is a common definition for WP, choosing different SST as criterion may lead to different characteristics of WP variation. For example, during boreal summer, the 29°C area index of WPWP falls obviously from May to June, while that of 28°C increases<sup>[15]</sup>. Recent work shows that high temperature warm water (HTWW) higher than 30°C in the South China Sea (SCS) shows up in

**Received** 2010-11-28; **Revised** 2011-12-04; **Accepted** 2012-01-15

**Foundation item:** National Natural Science Foundation of China (40975038, 40830106), National Basic Research Program of China (973 Program: 2012CB955604), Program from China Meteorological Administration (GYHY200906008), Project 111 (B07036)

**Biography:** HUANG Fei, Professor, primarily undertaking research on marine meteorology and air-sea interactions.

**Corresponding author:** HUANG Fei, e-mail: huangf@ouc.edu.cn

spring just before the onset of SCS summer monsoon (SCSSM), implying that the HTWW could be a good indicator for the onset of the SCSSM<sup>[16]</sup>. How do the characters of HTWW in WPWP behave, especially near the Philippine Sea—a core region of WPWP? This article discovers some interesting results of HTWW in WPWP by analyzing the frequency distributions of different WP SST during boreal summer and discusses the formation of this phenomenon.

Research has been done on the South China Sea (SCS) as part of WPWP. The impacts between summer monsoon and ocean there grab a lot of attention and have been studied extensively. Xie et al.<sup>[17]</sup> pointed out that the cold filament in SCS during summer is due to the upwelling caused by southwesterly monsoon wind impinging on Annam Cordillera. In their another work<sup>[18]</sup>, they showed that Philippine Islands and Annam Cordillera have similar impacts on the summer rainfall due to topographic effects.

However, there are only a few researches on the Philippine Sea. Maria et al.<sup>[19]</sup> discovers that an upwelling exists in Mindanao. It is caused by the cyclone circulation induced by the southern branch of the north equatorial current and the equatorial counter current, while this upwelling is actually relatively weak during the summer of Northern Hemisphere. It is proved later that it is not a key element for the variation of HTWW in the Philippine Sea. Sun et al.<sup>[20]</sup> pointed out that after the onset of southwest monsoon, the Ekman transport induced by surface winds makes the depth of the mixed layer shallow in the west and deep in the east of SCS. Does the topography of Philippine Islands have important effects, too? How does the monsoon affect the SST there? In this article, we are trying to answer these questions.

In the following sections, after introducing the data and analysis methods (section 2), we mainly discuss the inconsecutive frequency distributions of HTWW in the WPWP (section 3). Then we try to explain how this phenomenon forms (section 4) and its interannual change appears (section 5). Lastly, a summary and discussion is provided.

## 2 DATA

The high resolution Tropical Rainfall Measuring Mission (TRMM) SST daily data, with 0.25 by 0.25 degrees spatial resolution, is used here in this work for the period 1998 to 2008, which covers the entire ocean between 40°N and 40°S. For further analysis, the pentad mean data is calculated. Compared to the traditional SST dataset, the satellite microwave radiometers can measure SST through clouds, which is very useful because WP lies mainly in the tropical areas where convection activities occur frequently.

The microwave scatterometer, SeaWinds, launched on the QuikBird satellite (QSCAT), provides daily sea winds dataset from 2000 to 2008, with 0.25 by 0.25 degrees spatial resolution. The National Centers for Environmental Prediction/National Center for Atmospheric Research (NCEP/NCAR, USA) reanalysis provides daily 850 hPa winds dataset from 1998 to 2006 with 2.5 by 2.5 degrees spatial resolution. We also use the daily mean latent heat, sensible heat, net heat and short wave radiation dataset from WHOI (Woods Hole Oceanographic Institution) OAF flux (Objectively Analyzed air-sea Flux) project (<http://oafux.whoi.edu/index.html>), which is an ongoing research and development project for global air-sea fluxes<sup>[21]</sup>. Daily sea surface height (SSH) and ST are from SODA (Simple Ocean Data Assimilation) dataset<sup>[22, 23]</sup>. All the data described above are calculated on a pentad basis.

To analyze the variation of HTWW in WPWP, we first calculate the frequency distribution of different WP SST from 28°C to 30°C at 0.2°C intervals. In this article, the frequency of SST means the ratio of the pentads in which SST is higher than a certain value to the total pentads.

## 3 CHARACTERISTICS OF INCONSECUTIVE “SANDWICH STRUCTURE” PATTERN FOR HTWW IN THE WPWP

After investigating spatial frequency distribution of different WP SST, an inconsecutive high frequency distribution of SST in the WPWP is found when the WP SST is higher than 29°C, which mostly occurs in boreal summer. Figure 1 shows the seasonal variation of the spatially climatological frequency distribution of SST higher than 29.6°C. In boreal spring (MAM, Figure 1a), the warm pool is mainly located at the Southern Hemisphere, and the highest frequency lies near the date line. In boreal summer (JJA, Figure 1b), as the solar radiation moves northward, the high frequency distribution area moves northward, too. However, the high-frequency distribution of SST in the western Pacific is inconsecutive, which is blocked by a low-frequency distribution at the southeast of Philippine Islands (pane in Figure 1b). The relatively low-frequency area seems plugging into two high frequency regions in the north and southeast, which makes a “sandwich structure” pattern. Hereafter, we refer this inconsecutive distribution as a “sandwich structure”. In boreal autumn (SON, Figure 1c), as the direct solar radiation moves southward, the core of a high-frequency area also moves southward, meanwhile the “sandwich structure” disappears. In boreal winter (DJF, Figure 1d), the main body of the warm pool lies in the Southern Hemisphere again. It is worth noting that although the frequency distribution of different WP SST criteria are similar, the

“sandwich structure” cannot be observed in the spatial frequency distributions of SST lower than 29°C, implying that it is a special characteristic of HTWW. The “sandwich structure” also disappears in the

spatial frequency distributions of annual mean WP SST, suggesting that the phenomenon is season-dependent.

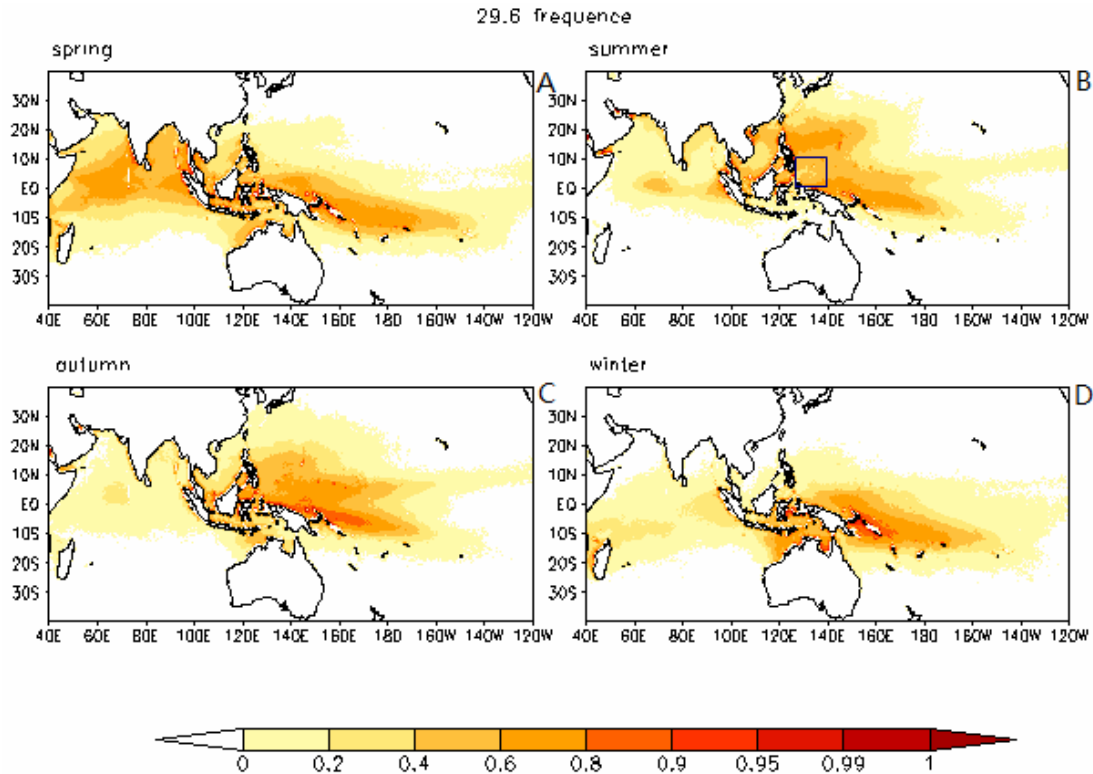


**Figure 1.** Climatological frequency distribution of SST higher than 29.6°C for spring (A), summer (B), autumn (C) and winter (D). The pane in the summer panel denotes the relatively low-frequency area plugging into two high frequency regions in the north and southeast, which makes a “sandwich structure” pattern.

The “sandwich structure” pattern also appears in summer SST fields in the western Pacific warm pool. The distribution of climatologically averaged sea surface wind stress and SST from May to October are shown in Figure 2. In May (Figure 2a), the main body of WPWP is located at the northern part of the Indian Ocean, part of the Philippine Sea and western Pacific, and monsoon occupies most of SCS, while trade winds prevail over the Philippine Sea. After that, SST in SCS decreases under the influence of monsoon, and southwesterly monsoon gradually affects the east of the Philippine Sea in June (Figure 2b), but the decrease of SST there is not obvious yet. Meanwhile, thanks to the northward movement of solar radiation, the core of the warm pool also moves northward, significantly increasing SST in the Philippine Sea but decreasing it in Indonesia. In July and August (Figures 2c & 2d), together with the onset of EASM, SST in SCS and Indonesia continues falling, and so does that in the southeast of Philippine Islands, which is corresponding to the “sandwich structure”. The inconsecutive frequency distribution of high SST appears. As southeasterly monsoon decays in September (Figure 2e), SST in the western Pacific

rises again, meanwhile the “sandwich structure” weakens. In October (Figure 2f), the “sandwich structure” disappears completely, but SST in SCS drops again with the onset of winter monsoon.

What is worth noting is that as the distribution of wind speed indicates (not shown), when EASM affects Philippine Islands in July, a wind jet is formed at the southern tip of it, which is probably the same reason behind the formation of the wind jet at the southern part of Annam Cordillera in boreal summer<sup>[17]</sup>. The core of wind speed is consistent with that of cold water in Figure 2c.

In summary, the “sandwich structure” exists only in boreal summer and reaches its peak in July and August, and all of this can only be observed in SST frequency distribution higher than 29°C. The phenomenon becomes more obvious when we pick higher SST as the criterion.

#### 4 FORMATION OF THE “SANDWICH STRUCTURE”

As observed above, the “sandwich structure” is most obvious in July and August when EASM

prevails over the same area (Figures 2c & 2d). Therefore, we mainly discuss whether EASM plays important roles in the formation of “sandwich

structure”, and how monsoon affects the SST, especially in the low-frequency distribution area.

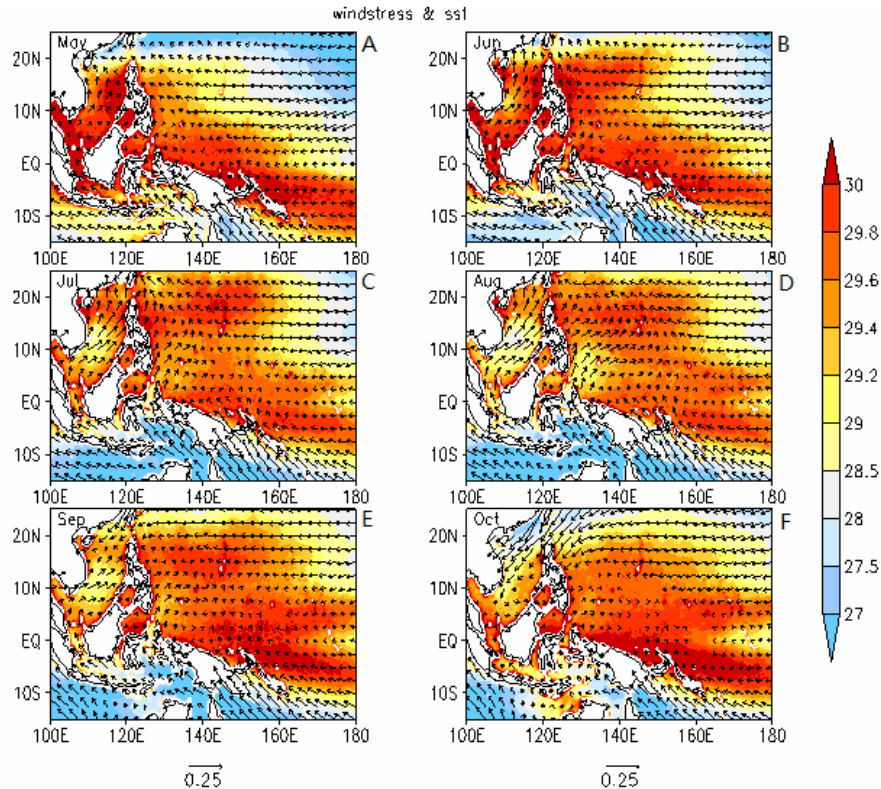


**Figure 2.** Spatial distribution of climatological mean SST and sea surface wind stress for May (A), June (B), July (C), August (D), September (E), and October (F). Shades are for SST (°C) and the arrow indicates sea surface wind stress ( $N/m^2$ ).

The WP area indices in Figure 3 show the size of an area where SST is higher than a certain value between  $130\text{--}140^\circ\text{E}$  and  $0\text{--}10^\circ\text{N}$ , with the area around indicated by a box in Figure 1b. The variations of pentad mean area indices from 1998 to 2008 (Figure 3a) as well as climatologically mean area indices (Figure 3b) are shown. Under the influence of EASM, the period of SCS WP area indices appears to be six months (figure omitted), because SST there decreases after the onset of EASM in May and recovers in October (Figures 2a & 2f). As expected, in Figure 3b, the WP area indices in the southeast of the Philippines also appear to have double-peak in a seasonal cycle. The “sandwich structure” shows up in June as the area indices decrease, which is remarkable when the SST chosen is higher than  $29^\circ\text{C}$  (the blue line), again implying that this is a special characteristic of HTWW. The variation of WP area indices southeast of the Philippines much resembles that for the SCS in July and August<sup>[17]</sup>, which indicates that EASM may also play important roles in the formation of the “sandwich structure”. The correlation of area indices in the two areas from July to August varies from 0.39 to 0.61, which increases as the SST picked as criterion rises. The correlation coefficients between the indices of SCSSM defined by Wang et al.<sup>[24]</sup> and the WP area

indices for  $130\text{--}140^\circ\text{E}$  and  $0\text{--}10^\circ\text{N}$  vary from  $-0.36$  to  $-0.60$ , decreasing as well as the SST rises. All of these imply that EASM may possibly affect the “sandwich structure” (Table 1).

Figure 4 illustrates how the  $30^\circ\text{C}$  WP area index (Figure 4a), precipitation (Figure 4b), latent heat flux (Figure 4c) and wind (Figure 4d)—averaged between  $0\text{--}10^\circ\text{N}$  and  $128\text{--}140^\circ\text{E}$ —are changing. Before analysis, we should mention that the variation of SST averaged in the same area resembles that of HTWW area index very much, which is very different from that of  $28^\circ\text{C}$  area index (Figure 3). In phase 1 and phase 2, the SST index varies ahead of precipitation and latent heat flux (affected by both precipitation and wind), and its mechanism is probably the same as HTWW in SCS in May<sup>[16]</sup>. As the area index of SST higher than  $30^\circ\text{C}$  rises dramatically in PS during boreal summer, the precipitation will increase due to the convection formed by HTWW. Later, the reduced solar radiation caused by precipitation will reduce the area of HTWW. This cloud-SST feedback was conducted by Ramanathan and Collins<sup>[25]</sup>. The peak of the HTWW area index lies in the first pentad in June before the feedback mechanism works, decreasing the index remarkably, an indication that the “sandwich structure” is formed.

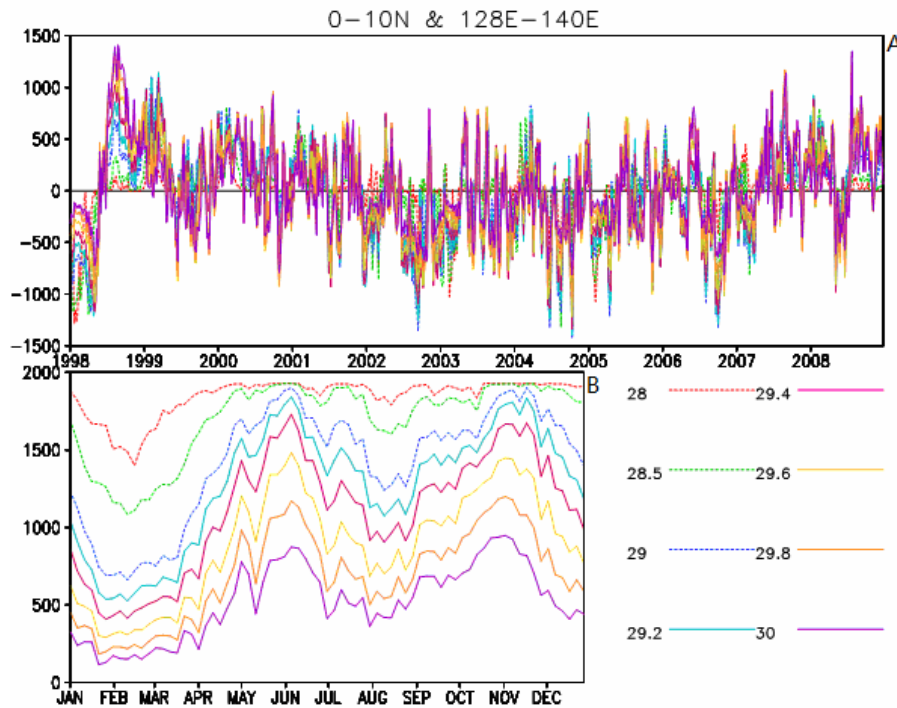


**Figure 3.** The variation of panted mean area indexes anomaly where SST is higher than a certain value from 28°C to 30°C in the area between 0–10°N and 128–140°E from 1998 to 2008 (A) and the climatologically averaged variation of area indexes (B).

**Table 1.** The correlation coefficients between the area indices in Figure 3 and SCS area indices when SST picked is higher than a certain value. The second column is for the correlation coefficients between the area indices in Figure 3 and SCSSM indices.

SST(°C)	Correlation coefficients of two area indices	Correlation coefficients between area indices and SCSSM indices
28	0.390	-0.358
28.5	0.408	-0.463
29	0.452	-0.569
29.2	0.502	-0.591
29.4	0.550	-0.603
29.6	0.592	-0.635
29.8	0.612	-0.624
30	0.611	-0.601

However, when the EASM reaches the PS area in July (phase 3 and phase 4), the speed of wind gradually increases. As a result, HTWW is then affected by both precipitation and wind, which can be clearly observed from the variation of latent heat flux. Especially in phase 4, the precipitation decreases dramatically to the same level with the beginning of phase 2, yet the HTWW area index only increases slightly. This may imply that during boreal summer, EASM plays a vital role in the maintenance of the “sandwich structure”.

All the discussions above indicate that EASM does have something to do with the formation of the

“sandwich structure”. Generally speaking, the winds affect the SST in two ways normally, one by affecting the latent heat, and the other by affecting the ocean circulation. That is why we discuss the roles of monsoon in the variation of SST in these two ways.

As shown in Figures 5c & 5d, the latent heat loss in July and August is indeed larger than in other months in the southeast of the Philippines (shown above), which seems to be caused by monsoon in that area. The same phenomenon can also be found in SCS. In the meantime, latent heat loss in the southeast of the Philippine Islands is larger than in the northern part, which is in favor of the formation of the “sandwich structure”. The difference between these two areas is identical to the distribution of wind speed, as the monsoon is largest in the southeast of Philippine Islands in July and August. However, the core of latent heat loss is located in the south of the low-frequency area, which means that their distributions do not coincide with each other exactly. This deviation may imply that latent heat loss is not the only reason (to be discussed later).

Figure 6 shows the variation of climatologically averaged latent heat (Figure 6a) and solar radiation (Figure 6b) averaged in three key areas of “sandwich structure”, including the low-frequency area we discussed before and the other two areas with high frequency in boreal summer. While the latent heat increases obviously from June to August in all three areas, solar radiation in the northern area is apparently higher than the other two areas in July and August,

which may be the reason why SST there is the highest. However, the red and green curves much resemble each other most of the time, but SST is lower in the central area than the southern, implying that the heat gain from the atmosphere still cannot explain the

difference between these two areas. As is well known, the South Equator Current transports warm water from Eastern Pacific to Western Pacific all year round<sup>[26, 27]</sup>, and this is probably why the SST of the southern part of WPWP in boreal summer is higher.

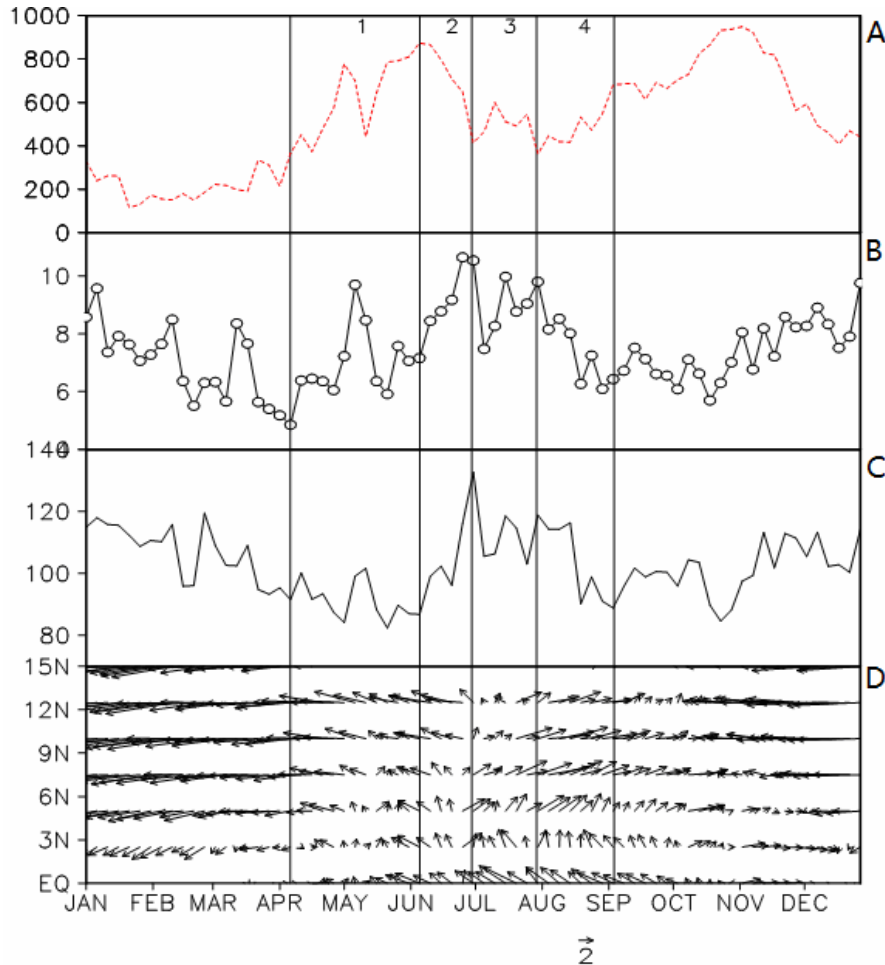


**Figure 4.** Climatological mean of the 30°C area index (A, red dashed line), precipitation (B, small circles) and latent heat (C, black line) averaged in the area between 0–10°N and 128–140°E. The arrow means the 850 hPa winds averaged between 0 and 10°N (D).

Then we focus on the other way by which winds affect the SST. Figure 7 shows the distribution of climatologically averaged ST from 5°S to 25°N and between 125°E and 130°E. We can tell by the plot that the upwelling in the southeast of Philippine Islands described earlier does exist, but it is very weak in boreal summer<sup>[19]</sup>. So it does no favor to the formation of the “sandwich structure”. As the solar radiation moves northward in summer, the ST between 5°S and 5°N falls obviously from July to September (Figures 4c & 4e). Meanwhile, southeast winds in the southern part and monsoon in the northern part help transport the cold water northeastward because of the Ekman transport and the distribution of SSH (Figure 8), which makes SST in the southwest of the Philippine Sea fall obviously, which is proved by the distribution of ocean currents in July and August (Figure omitted). This can also explain the deviation of the distribution between

latent heat loss and the low-frequency area. As a wind jet formed by EASM affects the southern tip of Philippine Islands, however, the decrease of SST only shows up in a small area. In a word, the decrease of SST in the southeast of Philippine Islands is local because of the topography.

## 5 INTERANNUAL VARIATION OF “SANDWICH STRUCTURE”

For further research, several special years are picked according to the time series of area indices in Figure 3a. In WP there is no remarkable cooling in the summers of 1998 and 2008, implying the “sandwich structure” may disappear, while the variation of SST in 2004 is very intense compared to normal years, indicating an extremely strong “sandwich structure” pattern in summer. Some studies have shown that there is a strong intraseasonal oscillation of monsoon

in 2004. After the onset of EASM, its strength weakened sharply in July and then recovered in August. In our research, the “sandwich structure” represents the similar characteristics, which means that the variation of SST in WP is identical to the monsoon. The same similarity also exists in the

summers of 1998 and 2008. During those years, under the influence of ENSO, EASM became weak<sup>[28]</sup>, and in the meantime, the “sandwich structure” disappeared. These cases prove the hypothesis that EASM is a key element in the formation of the “sandwich structure”.

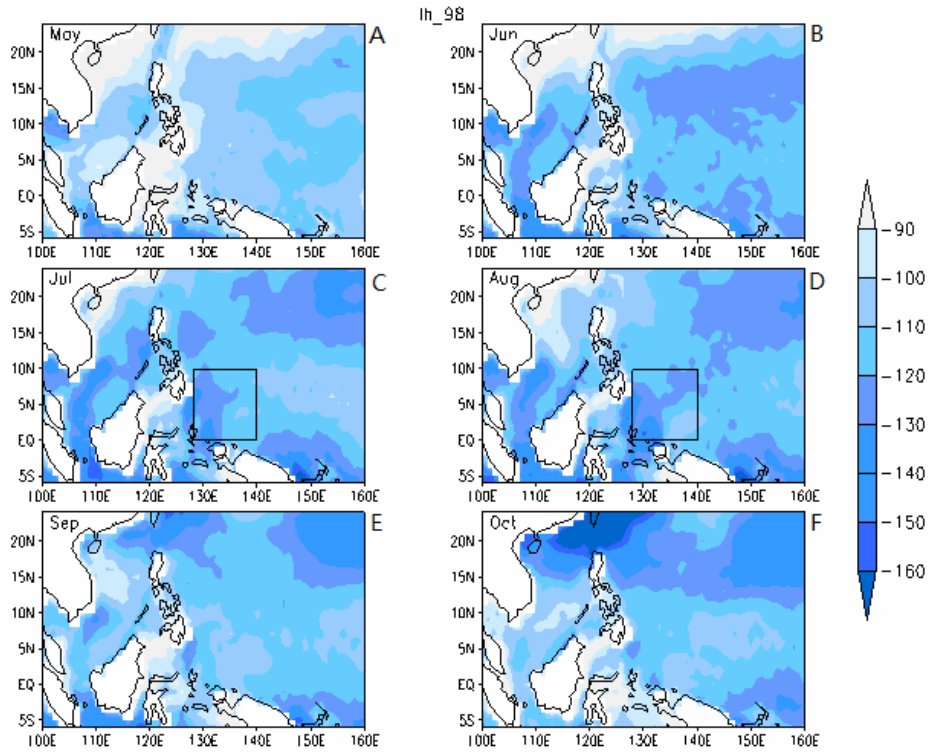


Figure 5. Same as Figure 2 but the shades are for latent heat.

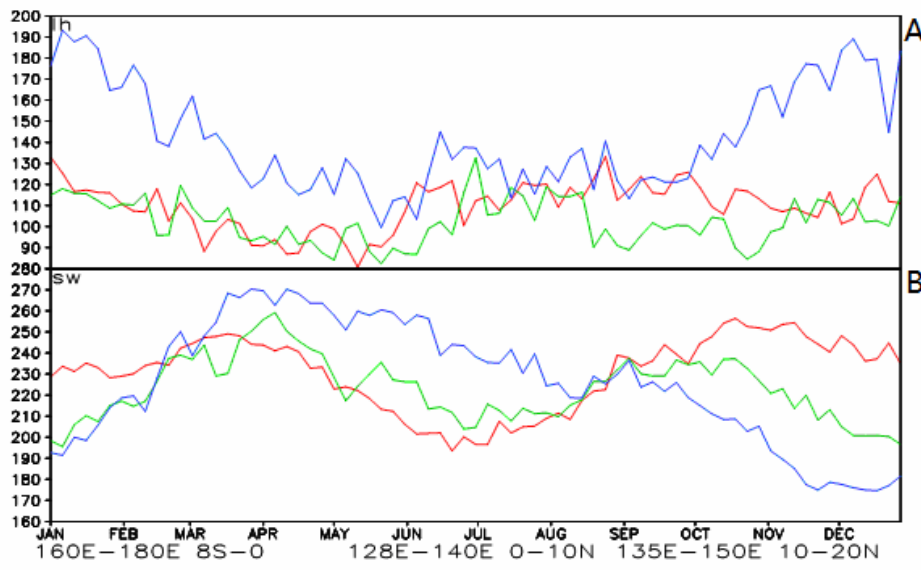
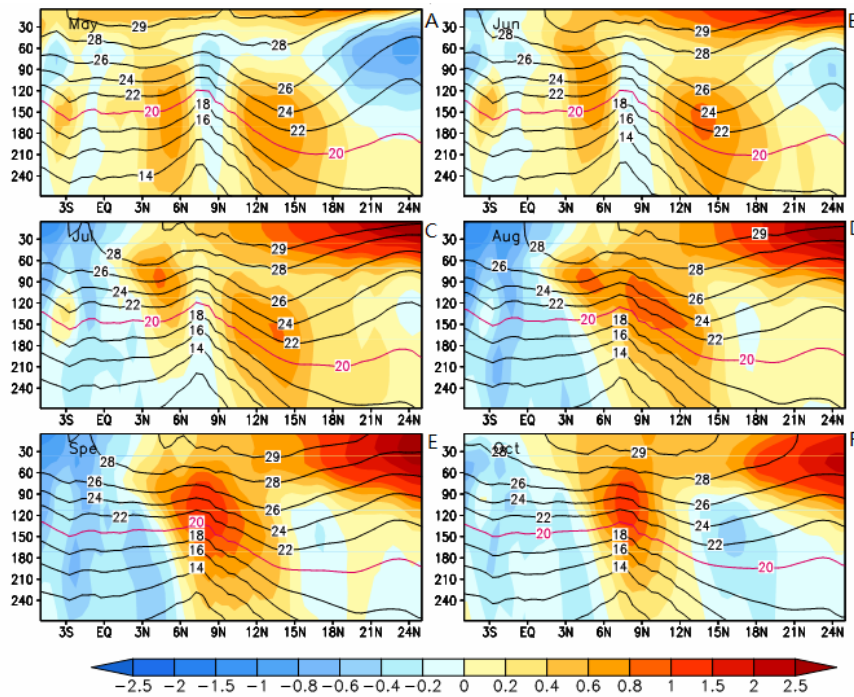
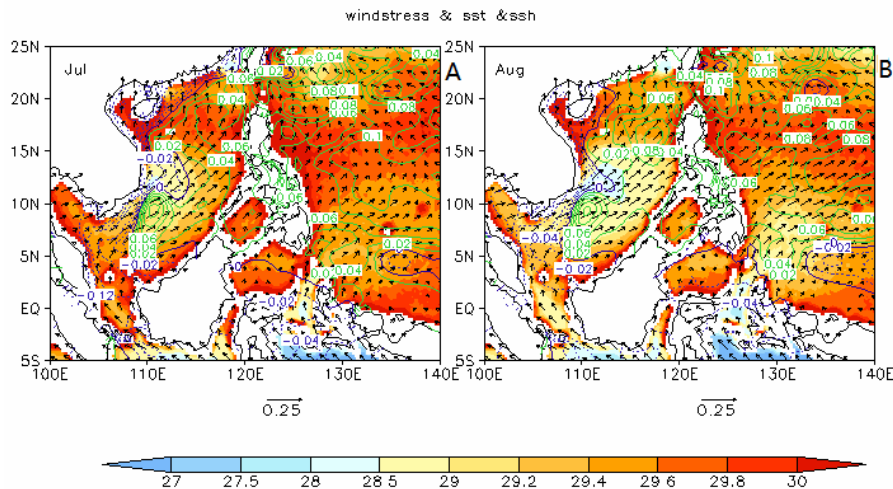


Figure 6. Time series of climatologically averaged latent heat (A) and solar radiation (B) in three key regions of the “sandwich structure”. The red line stands for the area between 8°S–0° and 160–180°E, the green line stands for the area between 0–10°N and 128–140°E, and the blue line for 10°S–20°N and 135–150°E.



**Figure 7.** Space distribution of climatically averaged ST and ST anomaly from May to October (A to F). Shading for STA, contours denote ST.



**Figure 8.** Space distribution of climatically mean SST, sea surface wind stress ( $N/m^2$ ) and SSH (m) in July (A) and August (B). Shading for SST, contours denote SSH, and arrow means sea surface wind stress.

In the meantime, in the special years we picked before, the variation of “sandwich structure” appears to be identical to latent heat loss, too (figures omitted).

### 6 CONCLUSIONS

The inconsecutive frequency distributions of high SST, which is caused by low SST in the southeast of Philippine Islands in boreal summer, known as the “sandwich structure”, does exist in the western Pacific warm pool. This phenomenon becomes more obvious when we pick higher SST as the criterion.

The low frequency in the Philippine Sea is possibly caused by southwest monsoon and sea water

transport together. In June, the precipitation at the southern tip of Philippine Islands increases dramatically because of the appearance of HTWW, which then causes the SST there to decrease obviously. Then as EASM affects the southern part of Philippine Islands in July, the latent heat loss there becomes larger, meanwhile the short-wave radiation decreases as the sunlit point of the Sun moves northward. As a result, the  $Q_{net}$  of the low-frequency area is smaller than in the northern part. On the other hand, thanks to the Ekman transport caused by winds, the cold water from the southern tip of Philippine Islands swarm northeastward. Eventually, the “sandwich structure” forms. As EASM retreats southward in September, the “sandwich structure”



weakens and disappears. Therefore, the summer monsoon does play an important role in the formation of the “sandwich structure”. In future research, we will focus on the role the “sandwich structure” plays in the climate variation in East Asia and Pacific Ocean.

Besides, several special years are picked based on the HTWW area indices in the low-frequency area. In these years, the variation of the “sandwich structure” coincides with that of EASM and latent heat very well.

## REFERENCES:

- [1] CHOU S H, ZHAO W, CHOU M D. Surface Heat Budgets and Sea Surface Temperature in the Pacific Warm Pool during TOGA COARE [J]. *J. Climate*, 1999, 13(3): 634-649.
- [2] WEBSTER P J, LUKAS R. TOGA COARE: The coupled ocean atmosphere response experiment [J]. *Bull. Amer. Meteor. Soc.*, 1992, 73(9): 1377-1416.
- [3] GRAHAM N E, BARNETT T P. Sea surface temperature, surface wind divergence, and convection over tropical oceans [J]. *Science*, 1987: 238(4827): 657-659.
- [4] HUANG Rong-hui, SUN Feng-ying. Impacts of the Thermal State and the Convective Activities in the Tropical Western Warm Pool on the Summer Climate Anomalies in East Asia [J]. *Sci. Atmos. Sinica*, 1994, 18(2): 141-151.
- [5] WANG B, WU R, FU X. Pacific-East Asian teleconnection: How does ENSO affect East Asian climate? [J]. *J. Climate*, 2000, 13(9): 1517-1536.
- [6] RAMANATHAN V, COLLINS W. Thermodynamic regulation of ocean warming by cirrus clouds deduced from observations of the 1987 El Niño [J]. *Nature*, 1991: 351(6321): 27-32.
- [7] FU R, DeL GENIO A D, ROSSOW W B, et al. Cirrus cloud thermostat for tropical sea surface temperature tested using satellite data [J]. *Nature*, 1992, 358(6385): 394-397.
- [8] WALLACE J M. Effect of deep convection on the regulation of tropical sea surface temperature [J]. *Nature*, 1992, 357(6375): 230-231.
- [9] HARTMANN D L, MICHELSEN M. Large-scale effects on the regulation of tropical sea surface temperature [J]. *J. Climate*, 1993, 6(11): 2049-2062.
- [10] LAU K M, SUI C H, CHOU M D, et al. An inquiry into the cirrus-cloud thermostat effect for tropical sea surface temperature [J]. *Geophys. Res. Lett.*, 1994, 21(12): 1157-1160.
- [11] PIERREHUMBERT R T. Thermostats, radiator fins and local runaway greenhouse [J]. *J. Atmos. Sci.*, 1995, 52(10): 1784-1806.
- [12] WANG B, LinHo. Rainy season of the Asian-Pacific summer monsoon [J]. *J. Climate*, 2002, 15(12): 386-398.
- [13] HOREL J D, WALLACE J M. 1981: Planetary-scale atmospheric phenomena associated with the Southern Oscillation [J]. *Mon. Wea. Rev.*, 109(4): 813-829.
- [14] WEBSTER P J. The role of hydrological processes in ocean-atmosphere interaction [J]. *Rev. Geophys.*, 1994, 32(4): 427-476.
- [15] LI Ke-rang, ZHOU Chu-ping, SHA Wan-ying. Basic feature of the warm pool in the western Pacific and its impact on climate [J]. *Acta Geograph. Sinica*, 1998: 53(?): 512-519 (in Chinese).
- [16] JIANG Xia, LIU Qin-yu, WANG Qi. Effects of warm water west of the Philippines on the South China Sea summer monsoon onset [J]. *J. Ocean Univ. China*, 2006, 36(3): 349-354 (in Chinese).
- [17] XIE S P, XIE Q, WANG D, et al. Summer upwelling in the South China Sea and its role in regional climate variations [J]. *J. Geophys. Res.-Oceans*, 2003, 108(3261): 1-37.
- [18] XIE S P, XU H M, SAJI N H, et al. Role of Narrow Mountains in Large-Scale Organization of Asian Monsoon Convection. *J. Climate*, 19(14): 2005: 3420-3429.
- [19] UDARBE-WALKER M J B, VILLANOY C L. Structure of potential upwelling areas in the Philippines. *Deep Sea Research Part I [J]. Oceanogr. Res. Papers*, 2001, 48(6): 1499-1518.
- [20] SUN X C, LIU Q Y, JIA Y L. Annual and interannual variations of the mixed layer in the South China Sea [J]. *J. Ocean Univ. of China*, 2007, 37(2): 197-203 (in Chinese).
- [21] YU L, WELLER R A. Objectively Analyzed air-sea heat Fluxes for the global OCE-free oceans (1981-2005) [J]. *Bull. Amer. Meteor. Soc.*, 2007: 88(4): 527-539.
- [22] CARTON J A, CHEPURIN G, CAO X, et al. A simple ocean data assimilation analysis of the global upper ocean 1950-1995, Part 1: methodology [J]. *J. Phys. Oceanogr.*, 2000, 30(2): 294-309.
- [23] CARTON J A, CHEPURIN G. A simple ocean data assimilation analysis of the global upper ocean 1950-1995, Part 2: results [J]. *J. Phys. Oceanogr.*, 2000, 30(2): 311-326.
- [24] WANG B, HO L, ZHANG Y S, et al. Definition of South China Sea monsoon onset and commencement of the East Asia summer monsoon [J]. *J. Climate*, 2004, 17(4): 699-710.
- [25] RAMANATHAN V, COLLINS W. Thermodynamic regulation of ocean warming by cirrus clouds deduced from observations of the 1987 El Niño [J]. *Nature*, 1991: 351(2): 27-32.
- [26] WYRTKI K. Geopotential topographies and associated circulations in the western South Pacific Ocean [J]. *Aust. J. Mar. Freshw. Res.*, 1962, 13(2): 89-105.
- [27] WYRTKI K. The subsurface water masses in the western South Pacific [J]. *Aust. J. Mar. Freshw. Res.*, 1962, 13(1): 18-47.
- [28] CESS R D, ZHANG M, WIELICKI B A, et al. The influence of the 1998 El Niño upon cloud-radiative forcing over the Pacific warm pool [J]. *J. Climate*, 2001, 14(9): 2129-2137.

**Citation:** HUANG Fei, ZHANG Lei, FAN Ting-ting et al. Inconsecutive “sandwich structure” pattern for high temperature warm water in the western Pacific warm pool. *J. Trop. Meteor.*, 2012, 18(1): 45-53.